ARTICLE

Carbon, Nitrogen, and Chalcogen Substitution Effects on 2,1,3-Benzothiadiazole Derivative: Theoretical Investigations of Electronic, Optical, and Charge Transport Properties

Bo Hu[a,b*], Chan Yao[a,b], Qing-wei Wang[a,b], Hao Zhang[c], Jian-kang Yu[c,d]

a. Faculty of Chemistry, Jilin Normal University, Siping 136000, China
b. Key Laboratory of Preparation and Applications of Environmental Friendly Materials, Jilin Normal University, Ministry of Education, Siping 13600, China
c. State Key Laboratory of Theoretical and Computational Chemistry, Jilin University, Changchun 130023, China
d. Institute of Applied Physics and Technology, The Foundation Department of Liaoning Technical University, Huludao 123000, China

(Dated: Received on September 8, 2011; Accepted on October 17, 2011)

A series of CH_2, NH, O, and Se substituted 2,1,3-benzothiadiazole derivatives have been designed and investigated computationally to elucidate their potential as organic light-emitting materials for organic light-emitting diodes. Both *ab initio* Hartree-Fock and hybrid density functional methods are used. It is found that adjusting the central aromatic ring by replacing S by CH_2, NH, O, and Se makes it possible to fine-tune the electronic, optical, and charge transport properties of the pristine molecule.

Key words: Organic light-emitting diode, 2,1,3-benzothiadiazole, Electronic property, Optical property, Reorganization energy

I. INTRODUCTION

During the past decades, many studies have focused on developing efficient and stable organic light-emitting materials [1−5]. The major method of tailoring the electronic, optical, and physical properties is through varying the molecular structures. To design an organic molecule with a specific application understanding the material structure-property relationship is necessary. Quantum chemical calculations can help providing structure-property relationships that are useful for the engineering of materials with improved characteristics.

We have previously taken a single-polymer white electroluminescent system (polyfluorene as a blue host and 2,1,3-benzothiadiazole (BTD)-based derivative as an orange dopant) as model compound to explore its experimentally observed electronic and spectroscopic behaviors employing the quantum-chemical calculations [6(a)]. Furthermore, a series of asymmetric derivatives were designed [6(b)] by introducing cyclopentadithiophene (CPDT) or fluorene to the backbone of 4,7-bis(4-(*N*,*N*-diphenylamino)phenyl)-2,1,3-benzothiadiazole [7, 8]. In this continuous investigation, {4-[7-(4,4-dimethyl-4*H*-cyclopenta[2,1−*b*;3,4−*b*′]dithiophen-2-yl)-benzo[1,2,5]thiadiazol-4-yl]-phenyl}-diphenyl-amine (OMC-PT, shown in Fig.1) and its electron-donating substituted derivatives are presented as potential candidates for orange dopants [6(b)].

The search for novel materials with promising structural and optoelectronic properties is still a challenge for scientists. In this work, on the basis of OMC-PT, four molecules with the different acceptor unit are chosen as the objects. The group X (shown in Fig.1) in the BTD core is varied along the same row (CH_2, NH, O) and the same group (O, S, Se). Modification of the BTD core by replacing S by CH_2, NH, O, and Se is expected to give rise to a new class of organic light-emitting materials. We applied the *ab initio* Hartree Fock (HF), density functional theory (DFT), configuration interaction singles (CIS), and time-dependent DFT (TD-DFT) methods to investigate the electronic, optical, and charge transport properties of these compounds. We attempt to gain better insights into the electronic, optical, and charge transport properties of these compounds to characterize the substituent effects

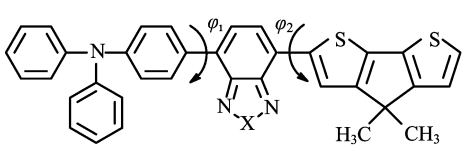

FIG. 1 Chemical structures of OMC-PT (X= S) and OMC-PT-X (X=CH_2, NH, O, and Se).

*Author to whom correspondence should be addressed. E-mail: hubo97@yahoo.cn

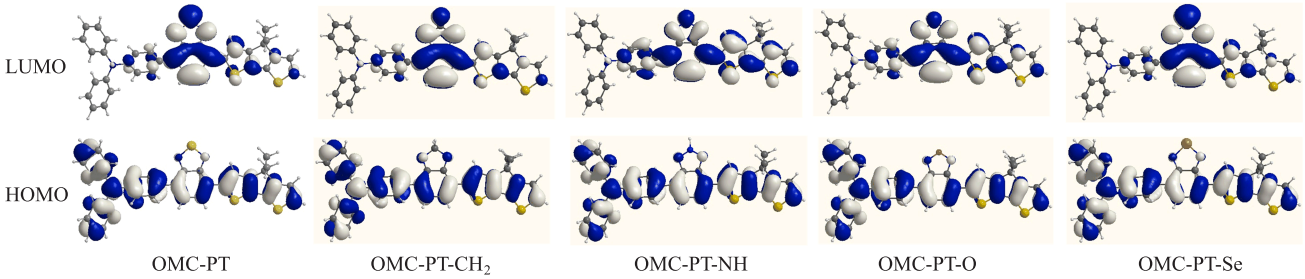

FIG. 2 HOMOs and LUMOs of OMC-PT and OMC-PT-X (X=CH_2, NH, O, and Se) calculated at the PBE0/6-31G(d)//HF/6-31G(d) level of theory.

on the optoelectronic properties using theoretical tools.

II. COMPUTATIONAL DETAILS

All calculations were performed with the Gaussian 03 package [9]. The methods applied in this work have been validated in our previous work [6(a)] and will be used in further analysis of optoelectronic properties in BTD-based derivatives. Geometry optimizations are performed for the ground-state (S_0) at the level of HF [10−12] and for the excited-state (S_1) using CIS approach [13]. Electronic properties are obtained based on the optimized S_0 geometries at the DFT [14] level by the PBE0 [15] hybrid functional. TD-DFT [16−18] is becoming the ideal method for treating the electronic absorption and emission spectra of medium to large organic molecules in recent years. On the basis of the optimized S_0 and S_1 geometries, the electronic absorption and emission spectra are calculated using TD-DFT with PBE0 functional, respectively. The above theoretical calculations are done with the 6-31G(d) [19−21] split valence polarized basis set. The reorganization energies are predicted from the single point energy at the B3LYP/6-31G(d,p) [19−21] level based on the PBE0/6-31G(d) optimized neutral, cationic, and anionic geometries.

III. RESULTS AND DISCUSSION

A. Electronic property

The analysis of the frontier molecular orbitals, that is, the highest occupied molecular orbitals (HOMOs) and the lowest unoccupied orbitals (LUMOs), can provide much useful information about a molecular reactivity. The electronic density distribution of the HOMOs and the LUMOs for OMC-PT and OMC-PT-X (X=CH_2, NH, O, and Se) are depicted in Fig.2. Characteristics similar to OMC-PT are observed for the HOMO and LUMO plots of OMC-PT-X (X=CH_2, NH, O, and Se). Their LUMOs mainly localized on substituted BTD, while their HOMOs mainly localized on triphenylamine (TPA) and CPDT.

Next we investigate the changes that take place upon CH_2, NH, O, and Se substitutions, to the frontier molecular orbitals, like the energies of the HOMO ($E_{\rm HOMO}$) and LUMO ($E_{\rm LUMO}$), HOMO-LUMO energy gap ($E_{\rm g}$). The $E_{\rm HOMO}$ and $E_{\rm LUMO}$ as well as the $E_{\rm g}$ for CH_2, NH, O, and Se substituted BTD-based derivatives based on OMC-PT are schematically plotted in Fig.3. The $E_{\rm HOMO}$, $E_{\rm LUMO}$, and $E_{\rm g}$ of the pristine molecule OMC-PT in S_0 lie at −5.18, −2.13, and 3.05 eV, respectively, while those in S_1 lie at −4.78, −2.43, and 2.35 eV, respectively. When S is replaced by CH_2 in BTD unit, the HOMO energy level is only slightly upshifted (−5.12 eV for S_0 and −4.71 eV for S_1) whereas the LUMO energy level is downshifted (−2.32 eV for S_0 and −2.60 eV for S_1) with the overall result of a smaller $E_{\rm g}$ (2.80 eV for S_0 and 2.11 eV for S_1). When S is replaced by NH in BTD unit, the HOMO (−5.09 eV for S_0 and −4.68 eV for S_1) and the LUMO (−1.57 eV for S_0 and −1.94 eV for S_1) energy levels are both upshifted, the more upshifted being the LUMO. A significant increasing $E_{\rm g}$ (3.52 eV for S_0 and 2.74 eV for S_1) is obtained in contrast to OMC-PT. From Fig.2 and Fig.3 it is noted that, substituents CH_2 and NH participate in their LUMOs, which could pronouncedly influence their $E_{\rm LUMO}$, while their HOMOs shows that no contribution from substituents CH_2 and NH, thus $E_{\rm HOMO}$ have no notable changes. On the other hand, O/Se substitution has only a minor effect on the $E_{\rm HOMO}$ (−5.24 eV for S_0 and −4.85 eV for S_1 in OMC-PT-O/ −5.16 eV for S_0 and −4.75 eV for S_1 in OMC-PT-Se), $E_{\rm LUMO}$ (−2.13 eV for S_0 and −2.44 eV for S_1 in OMC-PT-O/−2.21 eV for S_0 and −2.49 eV for S_1 in OMC-PT-O) and $E_{\rm g}$ (3.11 eV for S_0 and 2.41 eV for S_1 in OMC-PT-O/2.95 eV for S_0 and 2.26 eV for S_1 in OMC-PT-Se), which is ascribed to O, Se and S atoms belong to the same main group. Consequently, the affection of CH_2, NH, O, and Se substitutions towards the changing rate of $E_{\rm g}$ increases in the order: OMC-PT-CH_2<OMC-PT-Se<OMC-PT<OMC-PT-O<OMC-PT-NH both in S_0 and S_1.

B. Optical properties

The absorption and the emission spectra details (the vertical excitation energy $E_{\rm v}$, the maximum absorp-

DOI:10.1088/1674-0068/25/01/25-30

TABLE I Optical properties of OMC-PT and OMC-PT-X (X=CH_2, NH, O, and Se) computed at the TD-PBE0/6-31G(d) level.

	Absorption property			Emission property		
	E_v/eV	λ_{abs}/nm	f	E_v/eV	λ_{em}/nm	f
OMC-PT	2.50	496.4	0.54	1.94	639.4	0.83
OMC-PT-CH_2	2.26	548.8	0.61	1.72	720.6	0.79
OMC-PT-NH	2.99	414.7	1.17	2.40	515.7	1.58
OMC-PT-O	2.59	478.7	0.84	2.08	597.1	1.23
OMC-PT-Se	2.39	519.2	0.46	1.82	682.2	0.68

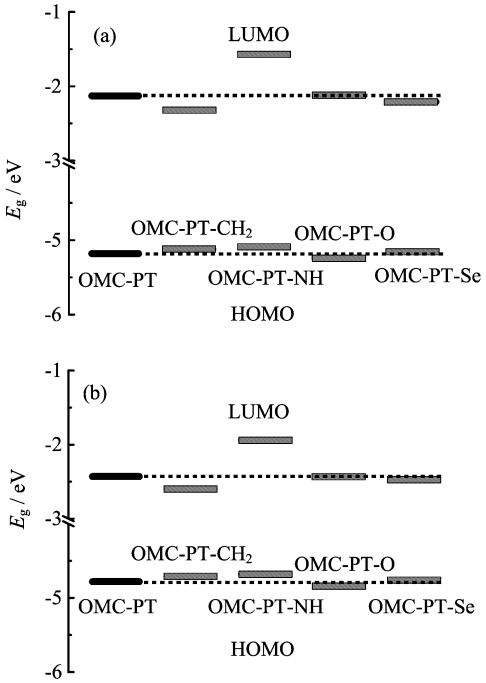

FIG. 3 Scheme of the frontier molecular orbital levels calculated at (a) the PBE0/6-31G(d)//HF/6-31G(d) level of theory and (b) the TD-PBE0/6-31G(d)//CIS/6-31G(d) level of theory.

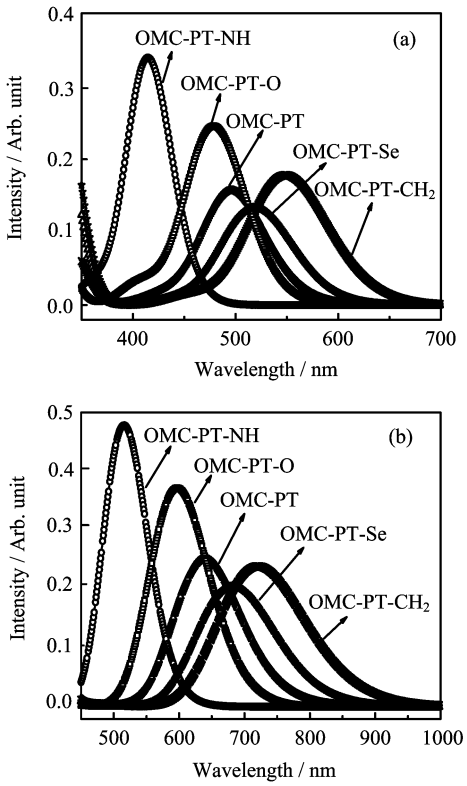

FIG. 4 (a) Absorption spectra and (b) emission spectra of OMC-PT and OMC-PT-X (X=CH_2, NH, O, and Se).

tion/emission wavelength $\lambda_{abs}/\lambda_{em}$ and corresponding oscillator strength f) for OMC-PT and OMC-PT-X (X=CH_2, NH, O, and Se) calculated by TD-DFT are collected in Table I. With respect to OMC-PT, on CH_2 and Se substitutions, λ_{abs} shows red shifted by 52.4 and 22.8 nm, respectively, whereas λ_{abs} of OMC-PT-NH and OMC-PT-O is blue-shifted by 81.7 and 17.7 nm, respectively. The same observation for λ_{em} is also found. Both the λ_{abs} and λ_{em} have the same variation trends with the decreasing order of OMC-PT-CH_2>OMC-PT-Se>OMC-PT>OMC-PT-O>OMC-PT-NH. Our calculations also show that the λ_{em} of OMC-PT-CH_2, OMC-PT-NH, OMC-PT-O, and OMC-PT-Se are located at the red, green, yellow, and red scope, so they may be used as red, green, yellow, and red light-emitting materials, respectively. It must be pointed out that the smaller E_g is, the more obvious the red shift in $\lambda_{abs}/\lambda_{em}$ is, and vice versa. Indeed, a remarkable correlation is found between E_g and $\lambda_{abs}/\lambda_{em}$ (shown in Fig.3 and Table I). Therefore, the change for $\lambda_{abs}/\lambda_{em}$ can be ascribed to the variation of E_g. What is very interesting is that, NH and O substitutions lead to marginally stronger oscillator strengths of the emission spectra with respect to OMC-PT, implying these two compounds could have larger fluorescent intensity and could be used as efficient green and yellow light-emitting materials, while in OMC-CH_2 and OMC-PT-Se it is lower than in OMC-PT, suggesting CH_2 and Se substitutions have no enhancing effect on the oscillator strength (shown in Table I and Fig.4).

The TD-DFT results shows that the electron excitation at the $\lambda_{abs}/\lambda_{em}$ is characterized as

DOI:10.1088/1674-0068/25/01/25-30

TABLE II φ_1 and φ_2 of OMC-PT and OMC-PT-X (X=CH_2, NH, O, and Se) in S_0 (HF/6-31G(d)) and S_1 (CIS/6-31G(d)).

	$\varphi_1/(^\circ)$			$\varphi_2/(^\circ)$		
	S_0	S_1	S_0-S_1	S_0	S_1	S_0-S_1
OMC-PT	44.96	23.62	21.34	25.24	−0.49	25.73
OMC-PT-CH_2	40.53	17.29	23.24	7.24	−0.26	7.50
OMC-PT-NH	41.31	21.83	19.48	19.97	−0.25	20.22
OMC-PT-O	39.97	15.55	24.42	13.86	−0.19	14.05
OMC-PT-Se	45.77	25.15	20.62	25.09	−0.61	25.70

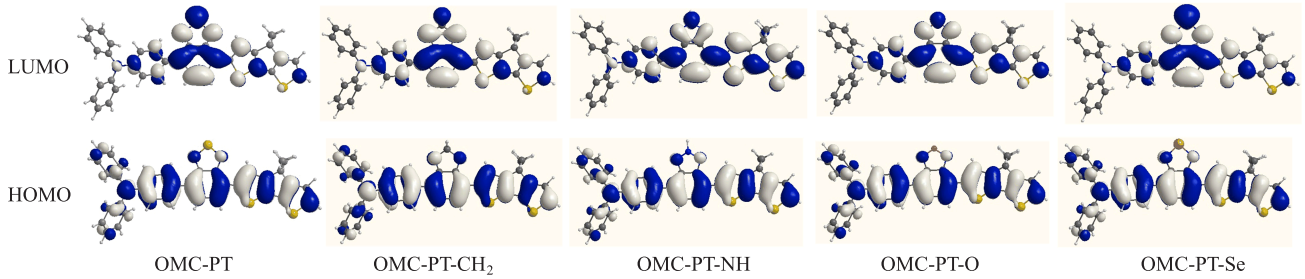

FIG. 5 HOMOs and LUMOs of OMC-PT and OMC-PT-X (X=CH_2, NH, O, and Se) calculated at the TD-PBE0/6-31G(d)//CIS/6-31G(d) level of theory.

HOMO→LUMO/LUMO→HOMO transition exclusively. The participating orbitals (HOMOs and LUMOs, Fig.2 and Fig.5) in the S_0 and S_1 show that, there are no notable changes in the LUMOs, and the orbital contribution is still mainly from the central BTD/substituted BTD as in the case of S_0. The distribution differences in the character of the HOMO comparing the S_0 and S_1 are much remarkable. In OMC-PT and OMC-PT-X (X=CH_2, NH, O, and Se), the contribution from the phenyl ring of BTD/substituted BTD, the spacer phenyl rings of TPA increase, whereas the contribution from another two phenyl rings of TPA decrease. A careful analysis of the optimized S_1 and S_0 geometries of the investigated derivatives gives important information on the dihedral angles φ_1 and φ_2 (Fig.1). For OMC-PT, the respective φ_1 and φ_2 values of 23.62° and −0.49° in S_1 are much smaller than the corresponding values of 44.96° and 25.24° in S_0. Similarly, for OMC-PT-X (X=CH_2, NH, O, and Se), the φ_1 and φ_2 values in S_1 are dramatically decreased with respect to the corresponding values in S_0 (shown in Table II). This indicates that S_1 geometries are favored to be more coplanar compared to those in S_0 ones. The decreasing dihedral angles may enhance the degree of π-conjugation between TPA/CPDT and BTD/substituted BTD. As a result, the HOMOs of OMC-PT and OMC-PT-X (X=CH_2, NH, O, and Se) are mainly localized on the phenyl ring of BTD/substituted BTD, the spacer phenyl rings of TPA, and CPDT. Moreover, large Stoke's shifts of 171.8 nm (OMC-PT-CH_2), 101.0 nm (OMC-PT-NH), 118.4 nm (OMC-PT-O), and 163.0 nm (OMC-PT-Se) also occur due to more planar conformations between TPA/CPDT and substituted BTD in S_1. The distribution patterns of the HOMOs and LUMOs present the charge transfer character in the absorption/emission transition.

C. Reorganization energy

The effect of the reorganization energy (λ_h/λ_e for hole/electron) in the charge transfer process is investigated because the reorganization energy has a dominant impact on the charge transfer rate. Here, the reorganization energy is just the internal reorganization energy of the isolated active organic π-conjugated systems due to ignoring any environmental relaxation and changes. Our calculations of the internal reorganization energy associated with different geometries of two states are based on the hopping model schematically illustrated in Fig.6. The internal reorganization energy corresponds to the sum of geometry relaxation energies upon going from the neutral state geometry to the charged state geometry and vice versa. The internal reorganization energy for hole transfer (λ_h) can be expressed as follows:

$$\begin{aligned}\lambda_h &= \lambda_{h0} + \lambda_{h+} \\ &= (E_0^* - E_0) + (E_+^* - E_+)\end{aligned} \quad (1)$$

As illustrated in Fig.6, E_0 and E_+ represent the energies of the neutral and cation species in their lowest energy geometries, respectively, while E_0^* and E_+^* represent the energies of the neutral and cation species with the ge-

DOI:10.1088/1674-0068/25/01/25-30

TABLE III Intramolecular reorganization energies (in eV) of OMC-PT and OMC-PT-X (X=CH_2, NH, O, and Se) computed at the B3LYP/6-31G(d,p)//PBE0/6-31G(d) level, which reorganize for hole and electron.

	λ_{h0}	λ_{h+}	λ_h	λ_{e0}	λ_{e-}	λ_e
OMC-PT	0.150	0.119	0.269	0.107	0.233	0.340
OMC-PT-CH_2	0.165	0.134	0.299	0.135	0.202	0.337
OMC-PT-NH	0.154	0.124	0.278	0.125	0.236	0.361
OMC-PT-O	0.148	0.112	0.260	0.114	0.241	0.355
OMC-PT-Se	0.160	0.133	0.293	0.105	0.223	0.328

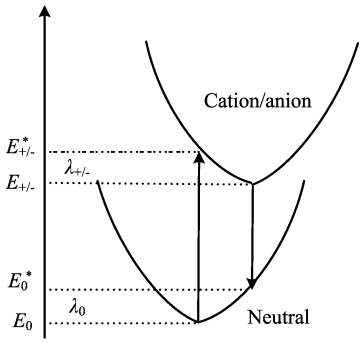

FIG. 6 Sketch of the potential energies of neutral and cation/anion species, illustrating the neutral (λ_0) and cation/anion ($\lambda_{+/-}$) relaxation energies.

ometries of the cation and neutral species, respectively. Electron transfer λ_e can be expressed as follows:

$$\begin{aligned}\lambda_e &= \lambda_{e0} + \lambda_{e-} \\ &= (E_0^* - E_0) + (E_-^* - E_-) \end{aligned} \quad (2)$$

The calculated λ_h and λ_e are listed in Table III. Theoretically, the calculated λ_h of OMC-PT-O is 9 meV lower than that of OMC-PT. It seems that O substitution decreases the λ_h. The calculated λ_h values of OMC-PT-CH_2, OMC-PT-NH, and OMC-PT-Se are higher than that of OMC-PT. Thus we conclude that CH_2 or NH or Se substitution has no positive effect on hole transportation. Herein, λ_h of OMC-PT-NH and OMC-PT-O are lower than that of typical hole transport material *N*,*N*′-diphenyl-*N*,*N*′-bis(3-methylphenyl)-(1,1′-biphenyl)-4,4′-diamine (TPD, λ_h=0.290 eV) [22], indicating their good hole transportation ability. The lower λ value is, the higher the charge-carrier transport rate is. The data show that λ_h values are all smaller than their respective λ_e, suggesting that the carrier mobility of the hole is larger than that of the electron for OMC-PT and OMC-PT-X (X=CH_2, NH, O, and Se) derivatives. It suggests that OMC-PT and OMC-PT-X (X=CH_2, NH, O, and Se) derivatives could be used as hole transport materials in the OLEDs from the stand point of its smaller reorganization energy. Furthermore, the difference between λ_h and λ_e for OMC-PT-CH_2 and OMC-PT-Se is only 0.038 and 0.035 eV, respectively, suggesting that these two compounds have better hole and electron transporting balance and could function as ambipolar charge transport materials.

IV. CONCLUSION

We report herein the implementation of a series of having varied structures to elucidate some of the relationships that may exist between the molecular structure and the optoelectronic properties. Comparison of CH_2, NH, O, and Se substituted compounds with OMC-PT shows that substituents CH_2, NH, O, and Se possess abilities to tune the electronic and optical properties of OMC-PT. The affection of CH_2, NH, O, and Se substitutions towards the changing of E_g increases in the order: OMC-PT-CH_2<OMC-PT-Se<OMC-PT<OMC-PT-O<OMC-PT-NH both in S_0 and S_1. Moreover, characteristics similar to OMC-PT are observed for the HOMO and LUMO plots of OMC-PT-X (X=CH_2, NH, O, and Se). Both the λ_{abs} and λ_{em} have the same variation trends with the decreasing order of OMC-PT-CH_2>OMC-PT-Se>OMC-PT>OMC-PT-O>OMC-PT-NH, which is ascribed to the variation of E_g. Also, OMC-PT-CH_2, OMC-PT-NH, OMC-PT-O, and OMC-PT-Se could function as red, green, yellow, and red light-emitting materials, respectively. Notably, NH and O substitutions lead to marginally stronger oscillator strengths of the emission spectra with respect to OMC-PT, implying these two compounds could have larger fluorescent intensity and could be used as efficient light-emitting materials. Finally, OMC-PT-X (X=CH_2, NH, O, and Se) may function as hole transport materials in the OLEDs on the basis of low reorganization energies of hole, and OMC-PT-CH_2 and OMC-PT-Se also could function as ambipolar charge transport materials. All the results indicate that CH_2, NH, O, and Se substitution of S in BTD core is a rational way toward good organic light-emitting materials.

V. ACKNOWLEDGMENTS

This work was supported by the Education Office of Jilin Province (No.2010142) and Institute Foundation of Siping City (No.2010009).

DOI:10.1088/1674-0068/25/01/25-30

[1] V. A. Montes, C. P. Bolvar, N. Agarwal, J. Shinar, and P. Anzenbacher Jr., J. Am. Chem. Soc. **128**, 12436 (2006).
[2] H. Namai, H. Ikeda, Y. Hoshi, N. Kato, Y. Morishita, and K. Mizuno, J. Am. Chem. Soc. **129**, 9032 (2007).
[3] H. Tsuji, C. Mitsu, Y. Sato, and E. Nakamura, Adv. Mater. **21**, 3776 (2009).
[4] H. Sasabe, J. I. Takamatsu, T. Motoyama, S. Watanabe, G. Wagenblast, N. Langer, O. Molt, E. Fuchs, C. Lennartz, and J. Kido, Adv. Mater. **22**, 5003 (2010).
[5] L. Duan, J. Qiao, Y. Sun, and Y. Qiu, Adv. Mater. **23**, 1137 (2011).
[6] (a) B. Hu and J. P. Zhang, Polymer **50**, 6172 (2009). (b) B. Hu, J. P. Zhang, and Y. Chen, Eur. Polym. J. **47**, 208 (2011).
[7] K. R. J. Thomas, J. T. Lin, M. Velusamy, Y. T. Tao, and C. H. Chuen, Adv. Funct. Mater. **14**, 83 (2004).
[8] S. I. Kato, T. Matsumoto, M. Shigeiwa, H. Gorohmaru, S. Maeda, T. Ishi-i, and S. Mataka, Chem. Eur. J. **12**, 2303 (2006).
[9] M. J. Frisch, G. W. Trucks, H. B. Schlegel, G. E. Scuseria, M. A. Robb, J. R. Cheeseman, J. A. Montgomery Jr., T. Vreven, K. N. Kudin, J. C. Burant, J. M. Millam, S. S. Iyengar, J. Tomasi, V. Barone, B. Mennucci, M. Cossi, G. Scalmani, N. Rega, G. A. Petersson, H. Nakatsuji, M. Hada, M. Ehara, K. Toyota, R. Fukuda, J. Hasegawa, M. Ishida, T. Nakajima, Y. Honda, O. Kitao, H. Nakai, M. Klene, X. Li, J. E. Knox, H. P. Hratchian, J. B. Cross, C. Adamo, J. Jaramillo, R. Gomperts, R. E. Stratmann, O. Yazyev, A. J. Austin, R. Cammi, C. Pomelli, J. W. Ochterski, P. Y. Ayala, K. Morokuma, G. A. Voth, P. Salvador, J. J. Dannenberg, V. G. Zakrzewski, S. Dapprich, A. D. Daniels, M. C. Strain, O. Farkas, D. K. Malick, A. D. Rabuck, K. Raghavachari, J. B. Foresman, J. V. Ortiz, Q. Cui, A. G. Baboul, S. Clifford, J. Cioslowski, B. B. Stefanov, G. Liu, A. Liashenko, P. Piskorz, I. Komaromi, R. L. Martin, D. J. Fox, T. Keith, M. A. Al-Laham, C. Y. Peng, A. Nanayakkara, M. Challacombe, P. M. W. Gill, B. Johnson, W. Chen, M. W. Wong, C. Gonzalez, and J. A. Pople, *Gaussian 03, Revision B.03*, Pittsburgh, PA: Gaussian Inc., (2003).
[10] C. C. Roothaan, J. Rev. Mod. Phys. **23**, 69 (1951).
[11] J. A. Pople and R. K. Nesbet, J. Chem. Phys. **22**, 571 (1954).
[12] R. McWeeny and G. J. Diercksen, Chem. Phys. **49**, 4852 (1968).
[13] J. B. Foresman, M. Head-Gordon, J. A. Pople, and M. J. Frisch, J. Phys. Chem. **96**, 135 (1992).
[14] R. G. Parr and W. Yang, *Density Functional Theory of Atoms and Molecules*, Oxford: Oxford University Press, (1989).
[15] (a) M. Ernzerhof and G. E. Scuseria, J. Chem. Phys. **110**, 5029 (1999). (b) C. Adamo and V. Barone, J. Chem. Phys. **110**, 6158 (1999).
[16] R. E. Stratmann, G. E. Scuseria, and M. J. Frisch, J. Chem. Phys. **109**, 8218 (1998).
[17] R. Bauernschmitt and R. Ahlrichs, Chem. Phys. Lett. **256**, 454 (1996).
[18] M. E. Casida, C. Jamorski, K. C. Casida, and D. R. Salahub, J. Chem. Phys. **108**, 4439 (1998).
[19] P. C. Hariharan and J. A. Pople, Mol. Phys. **27**, 209 (1974).
[20] M. S. Gordon, Chem. Phys. Lett. **76**, 163 (1980).
[21] M. J. Frisch, J. A. Pople, and J. S. Binkley, J. Chem. Phys. **80**, 3265 (1984).
[22] M. Malagoli and J. L. Brédas, Chem. Phys. Lett. **327**, 13 (2000).

DOI:10.1088/1674-0068/25/01/25-30